京都大学防災研究所年報　第44号 B-1　平成13年4月
Annuals of Disas, Prev. Res. Inst., Kyoto Univ., No.44 B-1, 2001

Experimental Study on the Shearing Behavior of Saturated Sandy Silts Based on Ring Shear Tests

Gonghui WANG, Kyoji SASSA and Takahiro TADA
Disaster Prevention Research Institute, Kyoto University, Kyoto, Japan

Synopsis

The shearing behavior of saturated silty soils has been studies extensively by performing drained and undrained ring shear tests on samples with different fine-particle contents. These samples were made by mixing loess into a fine-grained silica sand with 10, 20, 30, 50, and 70% loess by weight. By performing tests at different initial void ratios, the shear behavior of samples with different loess contents at loose and medium/dense states was presented and discussed. Undrained shear test results showed that both the peak and residual shear strengths decrease with increasing loess content. Meanwhile, by shearing the sample with different shear speed under naturally drained condition, the generation of pore pressure within the shear zone was analyzed. It is found that even in naturally drained condition, high pore water pressure could be built-up within the shear zone and kept for a long time with increasing in shear speed or fine-particle (loess) content on the sample.

Keywords: Shear resistance; Silty soils; Fine-particle content; pore water pressure; Ring-shear test

1. Introduction

A fluidized landslide is usually characterized by high mobility and long run-out distance, and then followed by tremendous hazards. It is always the result of liquefaction, a process during which high pore water pressure is generated and soil mass loses a great part of its strength and shows the behavior of liquid. Therefore, research on this kind of failure has been mainly focused on liquefaction potential analysis with emphasis on the undrained shear behavior of soils. By now there are countless experimental studies, which have been conducted on clean sand, and the undrained shear behavior of clean sand has been made relatively clear. However, compared with those tests on clean sand, the undrained shear behavior of silty soils is less studied, although it has been pointed out that silt and silt-clay mixture are more prone to suffer from liquefaction failure with long resultant run-out distance, basing on many field observations (Bishop, 1973; Eckersley, 1990; Ishihara, et al., 1990; Zlatovic and Ishihara, 1995). As stated by Guo and Prakash (1999), for evaluating the liquefaction potential of this kind of soil, there is no guideline available based on their density, void ratio, plasticity index, standard penetration values, or any other simple soil property; and even more, there is confusion on the influence of clay content, plasticity index, and void ratio. For example, by performing a series tests on loose samples prepared with varying percentages of both plastic and nonplastic fines and nonplastic fine sand, Pitman *et al.* (1994) found that undrained brittleness decreased as the fines content, for both plastic and nonplastic type, increased; at a fines content of 40% the stress path indicated only strain hardening towards steady state. Other research carried out by Ovando-Shelley and Perez (1997) had pointed out that within a limited range of clay content, the presence of clay increases the potential for generating

Table 1 Properties of employed samples, S7, S8, M10, M20, M30, and loess

Sample	S8	Loess	M10	M20	M30	M50	M70
Mean grain size, D_{50} (mm)	0.050	0.0185	0.047	0.043	0.040	0.032	0.025
Effective grain size, D_{10} (mm)	0.018	0.0012	0.0118	0.0084	0.0057	0.003	0.002
Uniformity coefficient, U_c	3.7	19.0	4.6	6.0	8.3	10.7	12.5
Maximum void ratio, e_{max}	1.66	–	1.51	1.52	1.56	–	–
Minimum void ratio, e_{min}	0.85	–	0.73	0.73	0.73	–	–
Specific gravity, G_s	2.63	2.72	2.64	2.65	2.66	2.68	2.70

Note: –: value was not measured.

excess pore pressure during undrained loading, and also reduces strength and stiffness.

From those researches mentioned above, it could be concluded that the undrained shear behavior of silty soils remains unclear and needs further extensive scrutiny. Therefore, in this research, to study those fluidized landsides where silty soils control the triggering and motion of landslide mass, ring shear tests were performed on a fine-grained sand and the mixtures of this sand with different loess by weight, under undrained or naturally drained (with the upper drainage hose of the shear box open) conditions. Based on the test results, the shearing behavior of silty soils was examined, and the mechanism of pore pressure generation within the shear zone was discussed and presented in this paper.

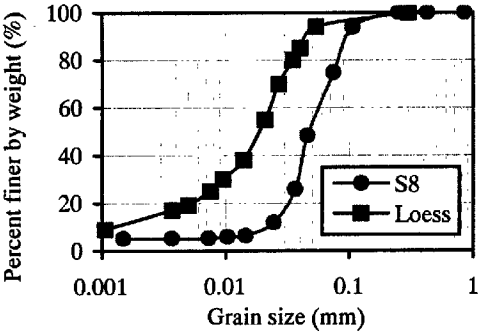

Fig. 1. Grain-size distributions of silica sand no. 8 and loess.

2. Sample Characteristics

In this research, silica sand no.8 (S8) was used as the sample. S8 is a uniform sandy silt composed of subangular to angular quartz. To study the shear behavior of silty soils with different grain size, loess was used also in this research. This loess, which was composed mainly of silt, was collected from a landslide at Lishan, Xi'an, China. In the present work, a series of tests was conducted on the mixtures of S8 and loess with loess content being 10, 20, 30, 50, and 70 percent, which were termed as M10, M20, M30, M50 and M70, respectively. The corresponding specific gravity for M10~M70 was calculated by weighted average. The grain-size distributions of S8 and loess are shown in Fig. 1, and some characteristics of the employed samples are listed in Table 1.

3. Test Apparatus and Test Procedure

3.1 Ring shear apparatus

Ring shear apparatus DPRI-Ver.6, developed and improved by Sassa and his colleagues after the 17 January 1995 Hyogoken-Nanbu earthquake, was used this research. This apparatus enables simulating all different kinds of static/dynamic loading and, has a large shear box sized 250 mm in inner diameter, 350 mm in outer diameter, and 150 mm in height. A detailed introduction on this ring shear apparatus could be referred to Sassa (1997, 2000). Here a section of half-side undrained ring shear box and the pore pressure measure system as well as the shear zone showing allspice-shaped cross section within the sample (formed in all the tests presented in this report) are illustrated briefly in Fig. 2.

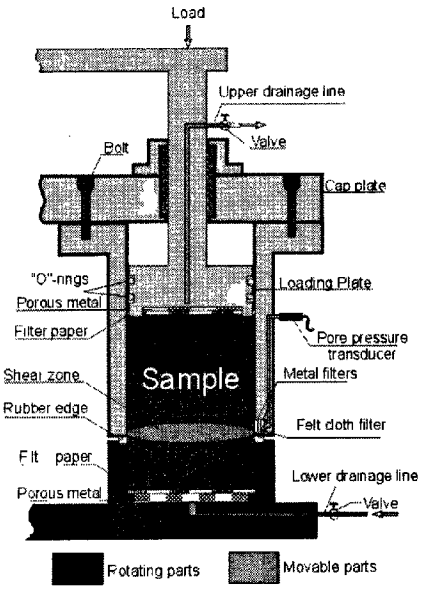

Fig. 2. Schematic illustration of the section of undrained shear box

3.2 Test procedure

The oven-dried sample was first set into the shear box, and then saturated with help of CO_2 and de-aired water. Thereafter, saturation degree was checked by B_D parameter, which was proposed by Sassa (1988) for the saturation degree in the direct shear state, and defined as the ratio between a normal stress increment (σ) and the resultant excess pore pressure increment (u), namely, $B_D = u/\sigma$. Because high saturation degree is necessary for acquiring correct monitoring data, in this study, all the tests were carried out with B_D 0.95.

All the samples were normally consolidated in this series tests under the pre-decided stress state. After the checking of B_D, the normal stress was decreased in undrained condition to a value (usually smaller than 49 kPa, due to the plasticity deformation nature of saturated sand) where the pore pressure decreased to zero, and then the upper drainage valve was switched to open. Thereafter, normal and then shear stresses were loaded slowly to the decided values. In the present research, all the samples were consolidated under the normal stresses of 196 kPa with no shear stress.

To allow more data to be sampled between the start point of shearing and the point where peak shear strength was mobilized, and then yield a well-defined effective stress path, torque-controlled method was selected in this research. Corresponding to the torque control, there are three kinds of rotating gear with final speed of Low (10 mm/sec), Medium (32.3 cm/sec) and High (2.25 m/sec). To avoid the phenomenon of runaway strains in contractive sand once the peak shear stress has been reached, which usually appears in stress-controlled triaxial compression tests, the Low gear was usually used for those undrained shearing tests, while both the Low and Medium gear were used for the drained shearing tests to study the influence of shear speed on the shear behavior of saturated soils under naturally drained condition. After consolidation, shear stresses were subsequently applied at a loading rate of 0.098 kPa/sec (0.001 kgf/cm^2/sec) under undrained condition or under naturally drained condition (by opening the upper drainage hose). Transducers were scanned at an interval of 1 second before the peak shear strength; after that, the sampling rate was increased to 20 samples/sec.

4. Test Results

Typical test results were selected to present the undrained shear behavior of different sample in different test conditions.

4.1 Undrained shear test

The effects of fine-particle contents (loess) content on the undrained shear behavior were examined in the loose state and dense state.

(1) In loose state

Because of the difficulties in making loose samples, the tests presented here to illustrate the effects of loess content on the undrained shear behavior were different in void ratio and initial normal stress. Nevertheless, the effects could be seen clearly through the tests results. Those selected tests results are plotted in Fig. 3 in the form of effective stress paths (ESP). The results of tests on S8 and M10, which are carried out under initial normal stress of 147 kPa with void ratios being 1.15 and 1.13 respectively, are selected to illustrate the effect of introduction of loess and shown in Fig. 3a. From this figure, it is seen that the ESP for S8 lies above that for M10, showing that both the peak and steady state shear strengths are greater than those of M10, although the void ratio of S8 is greater than that of M10. It is well known that for a sample under a certain initial stress state, these two strengths are the function of void ratio only; loose sample (greater in void ratio) has smaller peak and steady state shear strengths. Therefore, it could be concluded that these

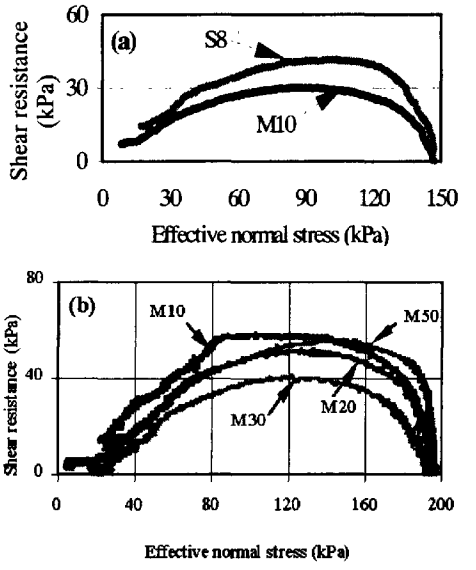

Fig. 3. Comparison of undrained shear behaviors of samples with different loess contents.
(a): Effective stress paths for S8 (e = 1.15) and M10 (e = 1.13); (b): Effective stress paths for M10 (e = 1.10), M20 (e = 1.02), M30 (e = 1.00), and M50 (e = 0.85).

differences are due to the introduction of loess.

Because of the difficulties in measuring the pore pressure within the shear zone especially for the tests on high silty soils, here just four tests on M10, M20, M30, and M50, which are performed under initial normal stress of 196 kPa with void ratio being 1.10, 1.02, 1.00, and 0.85, respectively, are used to interpret the influence of increasing loess content; and their results are presented in Fig. 3b in the form of effective stress path. As illustrated in this figure, the tests on M20, M30 and M50 showed collapse failure after the peak shear strengths were mobilized, while M10 behaved more like a sliding surface liquefaction failure: after the peak shear strength was mobilized, the shear resistance fell downward along the failure line with increasing shear displacement. Meanwhile, it is found that the both peak and residual shear strength (after sheared to 10 m) became smaller when loess content increased from 10% to 30%. The greater peak shear strength for M50 may due to the fact that M50 was the densest among these four tests.

(2) In dense state

Because no suitable test on dense S8 was obtained for this comparison in dense state, here tests results are just selected to illustrate the influence of increasing loess content on the undrained shear behavior. On the other hand, it is worth noting here that although efforts were made to get dense M50 and M70, by tamping the samples heavily, it did not work. After normally consolidated, the samples appeared no significant difference in the initial void ratios for the sample of M50, and M70, irrespective of the initial tamping. Therefore, we infer the s amples of M50 and M70 made by heavy tamping as "dense" state in this report. Because these two "dense" sample behaved almost the same as M30, here the results of tests on M10, M20, and M30 were presented in Fig. 4 to give a basic understanding on the effects of fine-particle (loess) content on the undrained shear behavior. The tests on M10, M20, and M30 were conducted with initial void ratios be 0.96, 0.89, and 0.89, respectively. The variation of shear resistance and pore pressure in relation to shear displacement are given in Figs. 4a, b, respectively; Fig. 4c shows the effective stress paths. As shown, with increasing loess content, the undrained shear behavior in the form of effective stress path changed remarkably. The test on dense M10 and M20 showed strong strain rehardening processes after the phase transformation point (point "PT"), during which shear strengths increased greatly due to suction of dense samples, and after failure, shear strengths reduced accompanying the generation of pore pressures (as presented in Figs. 4a, c) due to grain crushing. With increasing loess content, this strain rehardening process becomes weaker, showing a reduction in peak shear strength. For the test on dense M30, there was almost no rehardening process due to dilatancy. This tendency can be seen in Fig. 4b, where the pore pressure generation along with shear displacement showed a continuous increase throughout the whole shearing process without any temporary reduction. Meanwhile, the steady state shear strength becomes smaller with increasing loess content. Therefore, it is concluded that the undrained shear behavior was greatly affected by the fine-particle (loess) contents, by changing the peak and residual shear strengths.

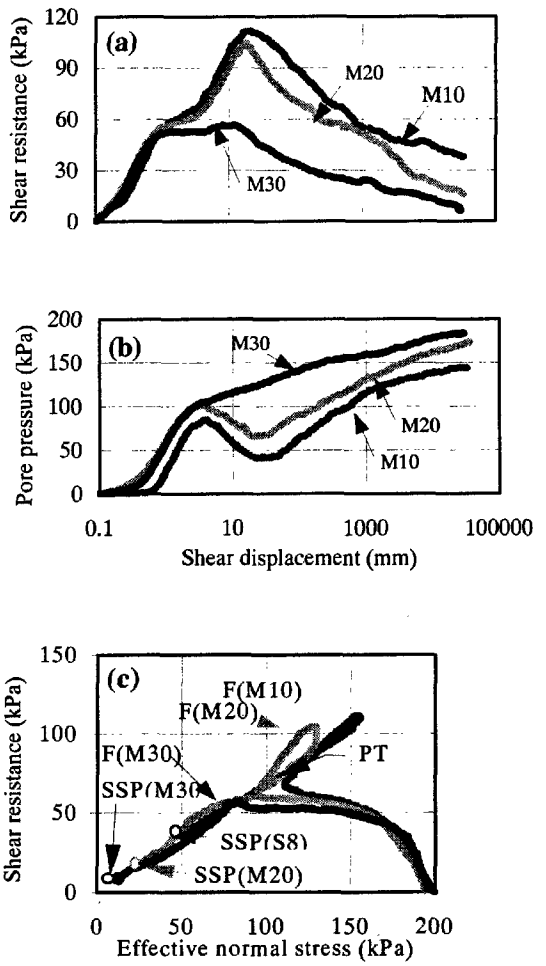

Fig. 4. Results of tests on M10, M20, and M30 in dense state (e = 0.96, 0.89, and 0.89 for M10, M20, and M30, respectively).
(a): Shear resistance against shear displacement;
(b): Pore pressure against shear displacement;
(c): Effective stress paths.

4.2 Naturally drained shear test results

In this series test program, the shearing on the saturated sample was performed with the upper drainage hose being open, namely, with permission of pore pressure dissipation. In this paper, naturally drained condition refers to this situation. In undrained condition, the effects of fine-particle (loess) content on the shearing behavior could be interpreted by the tests on M10, M30, and M50, and then in this naturally drained shearing test series, tests were performed on these three samples by using Low and Medium gears, respectively. In Low gear series tests, the shear displacement was 30 m, while that for Medium shearing tests were 100m. In the following, the shearing behavior in naturally drained condition is examined in loose and dense states for the tests in Low gear and Medium gear, respectively.

(1) In Low gear

These tests selected for interpreting the results of tests on M10, M20, and M30 in loose state were 1.10, 0.87, and 0.91 in void ratio. Figure 5 plotted the shear resistance against shear displacement. it is seen that although these three samples behaved the almost the same before reaching the peak shear strengths, the samples with greater fine-particle (loess) content showed greater reduction in shear strength after failure, irrespective of the naturally drained condition. This means that although the pore pressure is permitted to dissipate from the upper parts of the shear box, due to the formation of shear zone (as shown in Fig.2) in each test, pore pressure was built-up within the shear zone as the results of generation and dissipation. In fact, it could be inferred that with increasing fine-particle (loess) content, permeability decreases and the dissipation is retarded. This could be seen from Fig. 5b, where a relatively greater value of pore pressure was observed in the test on M50, although the monitored place is 2 mm above the shear zone, while almost no pore pressure was monitored for the tests on M10, and M30. Meanwhile, from Fig. 5a it is found that with progress of shear displacement, shear resistance recovered gradually for the tests on M10, and M30, while there was no recovery in shear strength for the test on M50, even when the shear displacement reached 30 m.

The similar phenomena were observed in the series tests on dense M10, dense M30, and "dense" M50, just as shown in Fig. 6, where the shear resistance (Fig. 6a) and monitored pore pressure (Fig. 6b) were plotted against shear displacement. Those tests selected for comparing the naturally drained

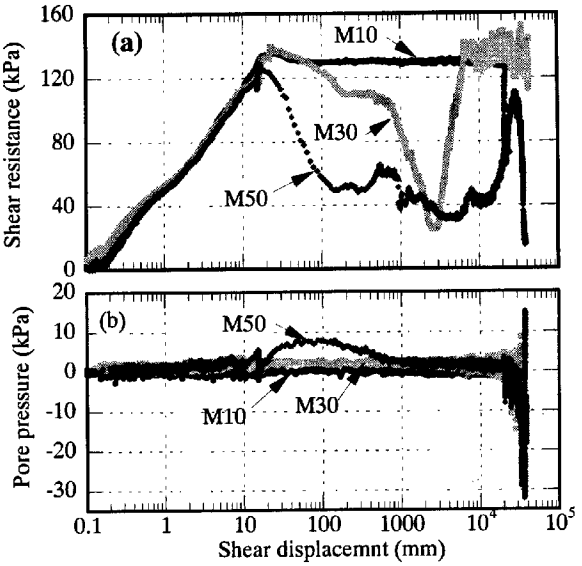

Fig. 5 Results of naturally drained shear tests (Low gear) on loose M10, M30, and M50 (e = 1.10, 0.87 and 0.91 for M10, M30, and M50, respectively).

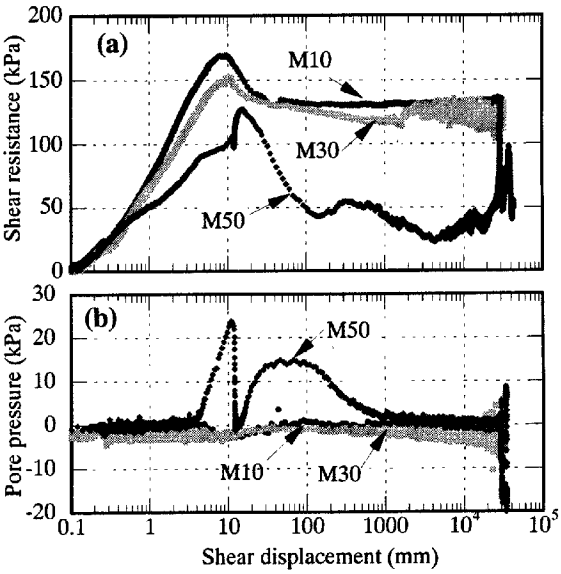

Fig. 6 Results of naturally drained shear tests (Low gear) on dense M10, dense M30, and "dense" M50 (e = 0.85, 0.81 and 0.83 for M10, M30, and M50, respectively).

condition were 0.85, 0.81, and 0.83 in void ratio for M10, M30, and M50, respectively. As shown in Fig. 6a, with increasing in fine-particle (loess) content, the peak shear strength became smaller, although the corresponding void ratio was becoming smaller (denser in normal sense). Meanwhile, the residual shear strengths for the tests on M10, and M30 showed no significant difference, while that for M50 was quite small. The monitored pore pressures for these three tests showed the same tendency: there was

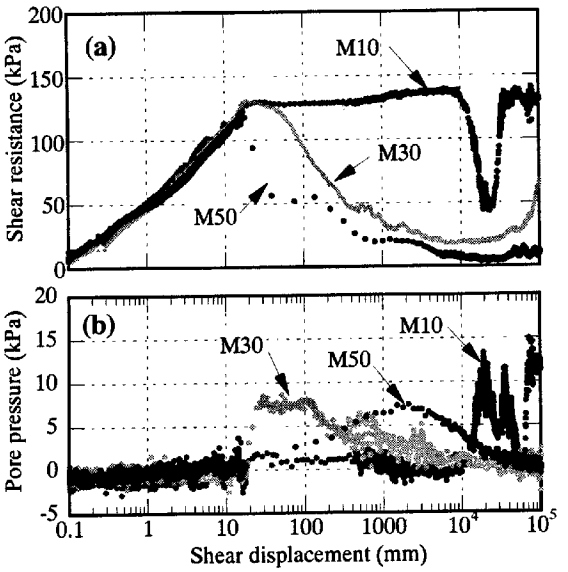

Fig.7 Results of naturally drained shear tests (Medium gear) on loose M10, M30, and M50 (e = 1.15, 1.03, and 0.95 for M10, M30, and M50, respectively).

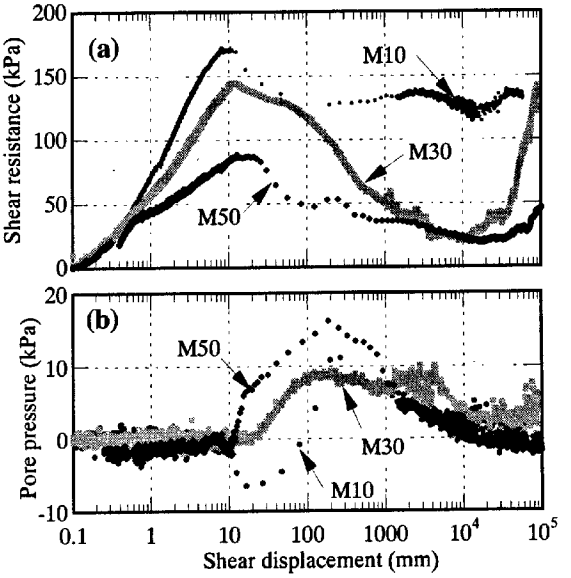

Fig.8 Results of naturally drained shear tests (Medium gear) on dense M10, dense M30, and "dense" M50 (e = 0.87, 0.87 and 0.89 for M10, M30, and M50, respectively).

almost no pore pressure recorded for the tests on M10, and M30, while M50 showed a great increase during shearing.

(2) In Medium gear

In this test series, all the samples were sheared to 100 m. Those tests selected for interpreting the results of tests on M10, M30, and M50 in loose state were 1.15, 1.03, and 0.95 in void ratio, respectively; and the results were presented in Fig. 7, where the shear strength (Fig. 7a) and monitored pore pressure (Fig. 7b) are plotted against the shear displacement. In this test series, these samples behaved almost the same before failure. Nevertheless, after failure, M30 and M50 showed great reduction in shear strengths, while M10 showed almost no reduction, although there was a temporary reduction in the shear process probably due to the built-up of pore pressure within the shear zone (it is seen that the monitored pore pressure showed temporary increase). It is very interesting to note that there was almost no recovery in the shear strength for test on M50, even when the sample was sheared to 100 m.

The variation of shear strength and monitored pore pressure in relation to the shear displacement for the tests on dense M10, dense M30, and "dense" M50 are presented in Figs. 8a, and b. The void ratios were 0.87, 0.87, and 0.89 for M10, M30, and M50, respectively. As shown in Fig. 8a, with increasing fine-particle (loess) content, the peak shear strength became smaller; and after failure, the shear strength of M10 keep almost the same, while those of M30 and M50 once reduced to a small value at the shear displacement of 10 m, and thereafter, the both of these two tests showed a recovering tendency with progress of shear displacement. Nevertheless, the shear strength of M30 recovered to a great value, while that of M50 was still kept small when the shear displacement reached 100 m. It is seen from Fig.8b that high pore water pressure was observed even in the test on dense M10, showing that the built-up of pore pressure could be affected greatly by the shearing speed after failure.

5. Test Results Discussions

5.1 Interpretation of results from undrained shearing tests

In dealing with the possible fluidization behavior of a soil mass in the field, the pore pressure generation process, peak shear strength and steady state strength may be the key parameters. Therefore, the different characterization of fluidization behavior of sands due to the change in fine-particle (loess) content will be examined in these three aspects.

(1) Undrained peak shear strength

For the tests carried out under the same initial stress state, the peak shear strength could reflect whether it is difficult for a given sample to suffer

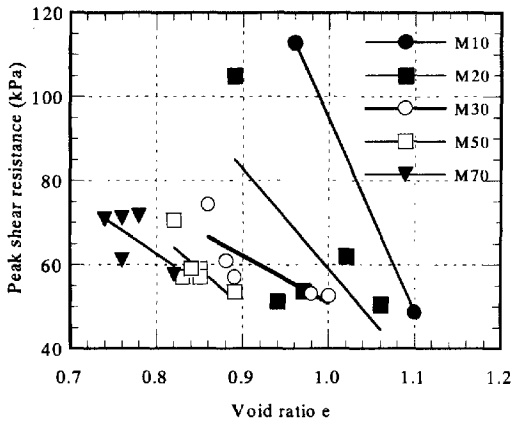

Fig. 9 Peak shear strength against void ratio for undrained shear tests.

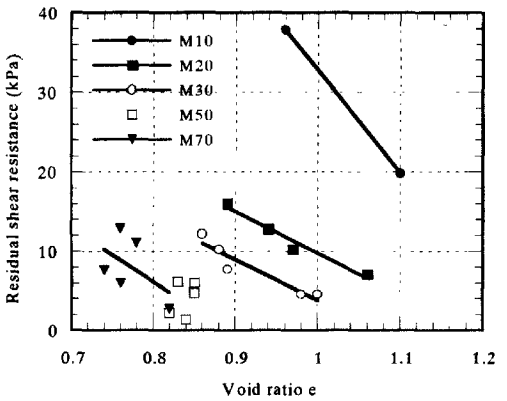

Fig. 10 Shear strength at steady state against void ratio for undrained shear tests.

fluidization failure or not. Therefore, emphasis was directed to the peak shear strength during the analysis of undrained shear behavior of samples with different fine-particle (loess) contents.

Because the peak shear strength is dependent on the initial stress state, here the peak shear strengths are all those tests carried out under the same initial stress state (initial normal stress = 196 kPa, and initial shear stress = 0). The peak shear strength for M10 ~ M70 were plotted in Fig. 9 against void ratio. As reflected in this figure, peak shear strength increases with decrease of void ratio (becoming denser) for each sample. From the changing trend of each sample, it could be seen that given the initial void ratio being the same, the peak shear strength becomes smaller with increasing fine-particle (loess) content (within the tested range of loess content of 70%).

(2) Steady state strength

Steady state strength plays an important role in

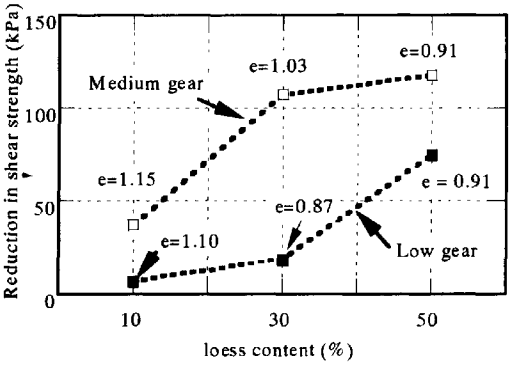

Fig. 11 Reduction in shear strength for sample with different loess content in naturally drained shear tests.

the motion of fluidized soil mass. It is directly related to the final slope angle when the fluidized mass stopped. As an important component in analyzing the fluidization behavior of sands with different fine-particle (loess) contents, here the steady state strengths are examined.

Figure 10 show the steady state points for all the tested samples, in the plane of void ratio versus τ_s plane, where τ_s is the shear strength at steady state. As shown, with increasing fine-particle (loess) content, the steady state line shifts the position from that of the M10; when the void ratio for each of them are the same, the shear strength at steady state becomes smaller with increasing fine-particle (loess) content, at least within the range of loess content being 70%.

5.2 Interpretation of results from naturally drained shearing tests

By now, most of the experimental studies on liquefaction were performed under undrained condition, although it was pointed out that undrained condition is not the prerequisite condition for liquefaction occurring. In fact, in many cases, especially those rainfall-induced fluidized landslides, high pore pressure was resulted after failure (during motion) and then the pore pressure generation and dissipation during motion will be two important factors affecting the built-up of pore pressure and then affecting the run-out distance.

As mentioned above, in the tests under naturally drained condition, different samples showed differing reductions in the shear strength after failure. Here this reduction (difference between the peak shear strength and the shear strength at the shear displacement of 30m (for Low gear) and 100 m (for Medium gear)) is examined for different tests. And the results are plotted in Fig. 11, where the abscissa shows the loess

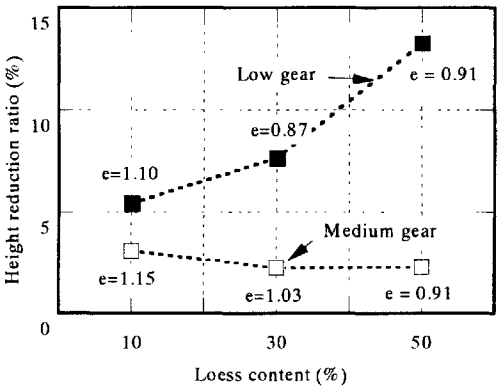

Fig. 12 Height change for sample with different loess content in naturally drained shear tests.

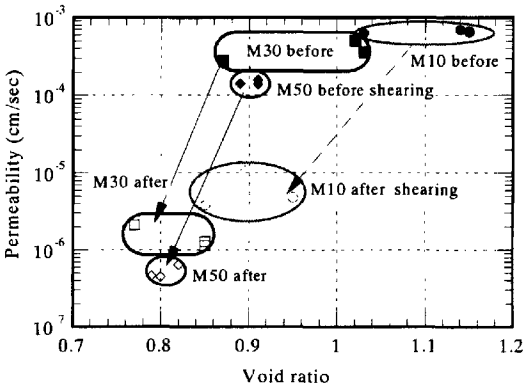

Fig. 13 Permeability against void ratio for naturally drained shear tests on M10, M30, and M50.

content in the sample, and ordinate presents the reduction in shear strength. It is seen that with increase of loess content in the sample, the reduction in shear strength became greater both for the Low gear and Medium gear tests. Meanwhile, Medium gear tests showed greater reduction in the shear strength than Low gear tests: the plots for Medium gear tests locate above these for Low gear tests. Therefore, it is concluded that in these naturally drained shear condition, the reduction in shear strength after failure depended on both the sample and the final shear speed after failure.

In undrained condition, it was pointed out that shear speed has no effects on the key results (Castro & Poulos, 1977). However, in these naturally drained ring shear tests, the generation of pore pressure is resulted from the volume shrinkage of the soil within the shear zone due to the collapse of unstable soil structures, the orientation of grains, and grain crushing (if the grains are crushable in the applied stress range), etc, with progress of shear displacement after failure. Dissipation of generated pore pressure is controlled by the permeability of the sample, and is time dependent. Because permeability of a sample is greatly dependent on the fine-particle content, it could be inferred that greater pore pressure could be built-up for the sample with greater fine-particle (loess) content, if the generated pore pressure is the same. On the other hand, faster final rotating speed means that the sample could be sheared to a greater displacement, providing the shear time being the same. In this sense, greater pore pressure could be generated due to the greater shear displacement, and then it is reasonable that greater pore pressure cold be built-up as the combined results of pore pressure generation rate and pore pressure dissipation rate.

The dissipation of generated pore pressure could be explained combining with the changes in sample's height. After the shear test was finished, the recorded sample height before failure (H_b) and that after shearing (H_f) were used to calculate the height reduction ratio ($\Delta H' = (H_b-H_f)/H_b$). And the height reduction ratios for those tests are plotted in Fig. 12 against the loess content in sample. It is seen that in the series tests using Low gear, the height reduction ratio became greater with increasing loess content in the sample, showing that the volume changing potential with shearing are becoming greater with increasing fine-particle (loess) content (at least within the tested loess content range of 70%). This showed good consistency with the results shown in Fig. 11, where M50 showed a greatest reduction in shear strength after failure within the three tests in Low gear. From Fig. 12, it is also seen that the height reduction ratio for the series tests in Medium gear became smaller with increase of loess content in the sample. As aforementioned, the pore pressure generation within the shear zone in this naturally drained shear condition was due to the collapse of unstable soil structures, grain orientation and grain crushing, etc.. If there were no dissipation of generated pore pressure from the shear zone, the volume of the sample should be kept the same and then there would have no change in sample height.

As stated above, the permeability of soil is a key parameter for the dissipation of pore pressure in the naturally drained shear tests. It is obvious that with increasing fine-particle (loess) content in the sample, the permeability becomes smaller. Meanwhile, the sample would become denser due to the volume shrinkage with progress of shear displacement. Grain crushing would result in the increase of fine-particle content in the shear zone, and then reduce the permeability further more. To examine the changes of

permeability of the soil within the shear zone in ring shear test, and then have a knowledge on the change of soil structures during shearing, permeability tests were performed before and after the naturally drained shear tests in Medium gear. During tests, de-aired water was flow into the shear box through the lower drainage hose, flow through the sample and, finally flow out through the upper drainage hose. During tests, a small water head was applied and steady. The measured permeability for different samples was presented in Fig. 13. It is seen that the permeability decreased significantly for all the samples after 100 m of shearing, and M50 showed smallest value. Meanwhile, it is found that though the permeabilities for all the samples before shearing located in the same order, after shearing, M50 showed significant reduction in permeability (about three orders), and the difference between M50 and M10 could be even in two orders. Because the permeability after shearing presented an average value, therefore, the soil within the shear zone would have a quite smaller permeability.

6. Summary and Conclusions

Several sets of ring shear tests were conducted on S8 and the mixtures of S8 with different loess content to study the shear behavior of sandy silt. Based on the tests results, the effects of fine-particle (loess) content on the shear behavior in both naturally drained and undrained conditions were examined. The conclusions could be drawn as follows.

(1) Sandy silty is highly liquefiable. In some tests on dense sample, there was no rehardening process during the undrained shearing process.

(2) With increase of fine-particle (loess) content, both the undrained peak and residual shear strengths became smaller.

(3) High pore pressure could be built up within the shear zone even in naturally drained condition. With increase of fine-particle (loess) content, the permeability decreases obviously and the greater pore pressure could be built-up within the shear zone. Meanwhile, it is revealed that this built-up of pore pressure depended greatly on the shear speed after failure. Fast motion after failure could result in great pore pressure generation and then reduction in the shear strength.

(4) The permeability could be reduced in three orders. After shearing, the sample with greater fine-particle (loess) content showed very small permeability. Due to this lowed permeability, high pore pressure could be built-up and kept within the shear zone, and than enable the rapid motion after failure. This finding provided an information or suggestion in the interpretation of some fluidized landslides with longer travel distance in fields.

Finally, it is worth noting that the shear behavior of silty soils is not very clear at present, and the test results presented here are quite limited. More detailed discussion on the pore pressure generation and dissipation as well as the effects of fine-particle (loess) content could be referred to Tada, T. (2001). Further studies on the synthetic effects of grain size and plastic fines on the shearing behavior of silty soils are needed and scheduled in the future.

Acknowledgements

The authors wish to thank Dr. Hiroshi Fukuoka, associate professor of Disaster Prevention Research Institute, Kyoto University, for his suggestions and discussions throughout this research.

References

Bishop, A.W. (1973). The stability of tips and spoil heaps. *Q.J. Engrg. Geol.* 6, 335-376.

Castro, G. & Poulos, S.J. (1977). Factors affecting liquefaction and cyclic mobility. *J. Geotech. Engrg. Div., ASCE.* 103, 501-516.

Eckersley, J. D. (1990). Instrumented Laboratory Flowslides. *Géotechnique* 40, No. 3, 489-502.

Guo Tianqiang & Shamsher Prakash. (1999). Liquefaction of silts and silt-clay mixtures. Journal of Geotechnical and Geoenvironmental Engineering, ASCE, Vol. 125, No. 8, pp. 706-710.

Ishihara, K., Okusa, S., Oyagi, N., & Ischuk, A. (1990). Liquefaction-induced flowslide in the collapsible loess deposit in Soviet Tajik. *Soils and Foundations* 30, No. 4, 73-89.

Ovando-Shelley, E., and B. E. Perez. (1997). Undrained behaviour of clayey sands in load controlled triaxial tests. *Géotechnique* 47, No. 1, 97-111.

Pitman, T. D., Robertson, P. K., and Sego, D. C. 1994. Influence of fines on the collapse of loose sands. *Can. Geotech. J.* Vol. 31, pp. 728-739.

Sassa, K. (1988). *Motion of Landslides and Debris Flows-Prediction of hazard area-.* Report for Grant-in-Aid for Scientific Research by Japanese Ministry on Education, Science and Culture (Project No. 61480062), pp.15.

Sassa, K. (1997). A new intelligent type of dynamic loading ring-shear apparatus. *Landslide News.* No.10, pp.33.

Sassa, K. (2000). Mechanism of flows in granular soils. Invited paper. *Proc. GeoEng2000*, Melbourne, **1**, 1671-1702.

Tada, T. (2001). *An experimental study on the mobility of landslides — Effects of fine-particle content on excess pore pressure built-up within the shear zone* —. Master Thesis, Kyoto University.

Zlatovic, S. and Ishihara, K. 1995. On the influence of nonplastic fines on residual strength. *Proc., IS-TOKYO'95, 1st Int. Conf. on Earthquake Geotech. Engrg.*, K. Ishihara, ed., A. A. Balkema, Rotterdam, The Netherlands, 239-244.

要旨

飽和された砂質シルトのせん断挙動を調べるために、シルト質の硅砂にレスを重量百分率で 10, 20, 30, 50, 70% 混合した試料に対し、非排水及び自然排水ﾘﾝｸﾞせん断試験を実施した．その結果、非排水状態において、ピークせん断強度と定常状態強度は、細粒部分の比率が高いほど小さくなる、そして、自然排水状態においては、低速・中速ギア両方で、細粒分含有率が大きい程、ピークせん断強度が減少した．また、100mまでの長距離せん断後のせん断強度は M10 では十分に回復しているのに対して、細粒分の多い M50 は低い値を維持した．細粒分の含有率、すなわち透水性の大小が粒子破砕による過剰間隙水圧の蓄積・発散特性に影響したためと考えられる．自然排水リングせん断試験（中速ギア）の試験前後で行った定水位透水試験の結果より、せん断後の透水係数はせん断前に比べて 3 桁低下した事がわかった．

キーワード：過剰間隙水圧、せん断抵抗、リングせん断試験、細粒分含有量、自然排水状態